be very interesting to assess the effect of pH variation and addition of SCN^- to the electrochemical and catalytic behavior of adsorbed cofacial CoP,[50-53] which appear to reduce O_2 to H_2O in an overall four-electron process.

The high conversion efficiency of O_2 to H_2O at favorable potentials by the cobalt porphyrins has served as the basis for a 200% efficient electrosynthesis cell where the cathodically generated H_2O_2 served as an effective oxidizing reagent.[28] Practical application of this, as well as other catalysts, will rely on long-term stability. Recent results on the question of catalytic stability suggested that a slow accumulation of CoP–oxygen or CoP–peroxy intermediates may be responsible for the gradual decay of activity of the adsorbed $Co^{III}TMPyP$ on the GCE. Attempts to identify such intermediates and to devise means of reactivation are currently under way and will be reported separately.

Acknowledgment. We gratefully acknowledge the financial support of this work by grants from the National Science Foundation and Koppers Company, Inc. (Pittsburgh, PA). The generous hospitality by T. Osa (Tohoku University) and K. Niki (Yokohama National University) to T.K., which allowed the writing of this paper during a professional leave, is greatly appreciated.

Registry No. $Co^{III}TMPyP$, 51329-41-0; $Co^{II}TMPyP$, 79346-65-9; $Co^{III}TMPyP(H_2O)_2$, 51405-04-0; $Co^{II}TMPyP(H_2O)_2$, 98064-63-2; $Co^{III}TMPyP(H_2O)(OH^-)$, 66114-42-9; $Co^{III}TMPy(OH^-)_2$, 98064-64-3; $Co^{III}TPyP(H_2O)_2$, 98064-65-4; $Co^{II}TPyP(H_2O)_2$, 98064-66-5; TPyP, 16834-13-2; H_2O_2, 7722-84-1; SCN^-, 302-04-5; O_2, 7782-44-7; H_2SO_4, 7664-93-9; C, 7440-44-0.

(50) Collman, J. P.; Morrocco, M.; Denisevich, P.; Koval, C.; Anson, F. *J. Electroanal. Chem. Interfacial Electrochem.* **1979**, *101*, 117.
(51) Collman, J. P.; Denisevich, P.; Konai, Y.; Morrocco, M.; Koval, C.; Anson, F. *J. Am. Chem. Soc.* **1980**, *102*, 6026.
(52) Durand, R. R., Jr.; Bencosme, C. S.; Collman, J. P.; Anson, F. *J. Am. Chem. Soc.* **1983**, *105*, 2710.
(53) Chang, C. K.; Liu, H. Y.; Abdalmuhdi, I. *J. Am. Chem. Soc.* **1984**, *106*, 2725.

Contribution from the Kenan Laboratories of Chemistry, The University of North Carolina at Chapel Hill, Chapel Hill, North Carolina 27514

Instability of the Oxidation Catalysts $[(bpy)_2(py)Ru(O)]^{2+}$ and $[(trpy)(phen)Ru(O)]^{2+}$ in Basic Solution

LEE ROECKER, WLODZIMIERZ KUTNER,† JOHN A. GILBERT, MIRIAM SIMMONS,§ ROYCE W. MURRAY, and THOMAS J. MEYER*

Received January 14, 1985

The Ru(IV) complexes $[(bpy)_2(py)Ru(O)]^{2+}$ (**1**) and $[(trpy)(phen)Ru(O)]^{2+}$ (**2**) (bpy = 2,2′-bipyridine, py = pyridine, trpy = 2,2′,2″-terpyridine, and phen = 1,10-phenanthroline) are unstable toward self-reduction in basic solution. Product analyses, performed by using UV–vis spectroscopy, cyclic voltammetry, HPLC, and GC, show that O_2 is not a product of the self-reductive chemistry and that ca. 80% of the reduced products that appear are the unmodified polypyridyl complexes of Ru(II), $[(bpy)_2(py)Ru(OH)]^+$ or $[(trpy)(phen)Ru(OH)]^+$. The remaining 20% of the products are accounted for by at least four different products, which are also Ru(II) but appear to have undergone varying degrees of ligand oxidation. Kinetic studies were performed with stopped-flow or conventional mixing techniques. For complex **2**, plots of log $|A_\infty - A_t|$ vs. time were linear from pH 12 to 14 and the experimental rate law can be described by $-d[Ru(IV)]/dt = k_a[OH^-] + k_b[OH^-]^2$, where $k_a = 0.21 \pm 0.01\ M^{-1}\ s^{-1}$ and $k_b = 0.08 \pm 0.02\ M^{-2}\ s^{-1}$ at 25 °C and $\mu = 1.0$ M (Na_2SO_4). For the k_a path $\Delta H^\ddagger = 12 \pm 2$ kcal/mol and $\Delta S^\ddagger = -20 \pm 6$ eu. For complex **1**, plots of log $|A_\infty - A_t|$ vs. time were not linear but could be resolved into two successive components to yield rate constants for the self-reduction of Ru(IV) and, following that, of Ru(III). The differences in behavior in basic media between complexes **1** and **2**, and possible mechanistic schemes for the self-reduction, are discussed as are possible implications of the ligand-based redox chemistry for utilization of the ruthenium oxo complexes as oxidation catalysts in basic solution.

Polypyridyl complexes containing the $Ru^{IV}{=}O$ group have been observed to act as stoichiometric or catalytic oxidants for a variety of organic and inorganic substrates.[1-9] A potentially important variable in using these reagents as oxidants is pH. For example, while acetone is virtually unreactive toward $[(trpy)(phen)Ru(O)]^{2+}$ in acidic solution ($k < 10^{-6}\ M^{-1}\ s^{-1}$ at pH 2), oxidation of acetone is rapid in basic solution ($k = 8.75\ M^{-1}\ s^{-1}$ at pH 13).[9]

Although aquo or hydroxo polypyridyl complexes of Ru(II) are stable at any pH, higher oxidation states are somewhat unstable in basic media toward self-reduction to Ru(II). Ghosh et al.[10] have noted that the instability of $[Ru(bpy)_3]^{3+}$ toward spontaneous reduction in basic solution occurs, at least in the first stage, by oxidative hydroxylation of the polypyridyl ligands. Nord, et al.[11] have proposed that the spontaneous decay of Fe(III) polypyridyl complexes leads to Fe(II) complexes and coordinated, ligand-based *N*-oxides as primary products.

We have investigated and report here the results of a series of studies on the instabilities of $[(trpy)(phen)Ru(O)]^{2+}$ and $[(bpy)_2(py)Ru(O)]^{2+}$ in basic solution toward self-reduction. It is an important study from our point of view because the possibility of developing selective functional group oxidation schemes based on Ru–oxo complexes depends, in part, on an ability to utilize pH variations, and therefore, it is necessary to define the pH regions of catalyst stability.

Experimental Section

Materials. Reagent grade $(NH_4)_2[Ce(NO_3)_6]$ (G. F. Smith Chemical Co.) was used to prepare solutions of Ce(IV), which were standardized spectrophotometrically at 320 nm ($\epsilon = 1320\ M^{-1}\ cm^{-1}$). 2-Hydroxypyridine and 1,10-phenanthroline (Aldrich Chemical Co.) were used without further purification. The electrolyte, $[(C_2H_5)_4N](ClO_4)$(TEAP), used in electrochemical measurements was recrystallized twice from H_2O

† On leave from the Institute of Physical Chemistry, Polish Academy of Sciences, 01-224 Warsaw, Poland.
§ Present address: Technology Enterprises Division/3M, 219-1-01 3M Center, St. Paul, MN 55144.

(1) Meyer, T. J. *J. Electrochem. Soc.* **1984**, *131*, 221C.
(2) Samuels, G. J.; Meyer, T. J. *J. Am. Chem. Soc.* **1981**, *103*, 307.
(3) McHatton, R. C.; Anson, F. C. *Inorg. Chem.* **1984**, *23*, 3935.
(4) (a) Thompson, M. S.; De Giovani, W. F.; Moyer, B. A.; Meyer, T. J. *J. Org. Chem.* **1984**, *49*, 4972. (b) Moyer, B. A.; Thompson, M. S.; Meyer, T. J. *J. Am. Chem. Soc.* **1980**, *102*, 2310.
(5) Thompson, M. S.; Meyer, T. J. *J. Am. Chem. Soc.* **1981**, *103*, 5070.
(6) Thompson, M. S.; Meyer, T. J. *J. Am. Chem. Soc.* **1982**, *104*, 4106.
(7) Kutner, W.; Meyer, T. J.; Murray, R. W. *J. Electroanal. Chem. Interfacial Electrochem.*, in press.
(8) Roecker, L.; Meyer, T. J., submitted for publication.
(9) Roecker, L.; Kutner, W., unpublished results.
(10) Ghosh, P. K.; Brunschwig, B. S.; Chou, M.; Creutz, C.; Sutin, N. *J. Am. Chem. Soc.* **1984**, *106*, 4772.
(11) Nord, G.; Pedersen, B.; Bjergbakke, E. *J. Am. Chem. Soc.* **1983**, *105*, 1913.

0020-1669/85/1324-3784$01.50/0

and vacuum-dried. All other reagents were of reagent quality and used without further purification. Elemental analyses were performed by Galbraith Laboratories, Knoxville, TN.

Syntheses. The preparations of $[(bpy)_2(py)Ru(H_2O)](ClO_4)_2$, $[(bpy)_2(py)Ru(O)](ClO_4)_2$, and $[Ru(trpy)Cl_3]$ have been described.[12,13]

[(trpy)(phen)RuCl]PF_6 was prepared by heating 3.00 mmol (132 mg) of $[Ru(trpy)Cl_3]$, 3.00 mmol (541 mg) of 1,10-phenanthroline, and 30.0 mmol (127 mg) of LiCl at reflux for 30 min in 270 mL of 3/1 ethanol/water under a N_2 atmosphere. After 30 min, the solution was cooled and the volume reduced to ca. 80 mL. Saturated NH_4PF_6 was then added and the solution chilled. The resulting brown solid was collected on a fritted funnel and air-dried. The solid was purified by elution from an alumina column with 1/2 toluene/acetonitrile. The first red-brown band eluted is the desired product with $E^{\circ\prime} = 0.8$ V vs. SSCE in 0.1 M TEAP/acetonitrile for the Ru(III)/Ru(II) couple. Yield: 400 mg; 19.3%.

[(trpy)(phen)Ru(H_2O)]$(ClO_4)_2$ was prepared by dissolving 0.47 mmol (330 mg) of [(trpy)(phen)RuCl]PF_6 and 1.00 mmol (207 mg) of $AgClO_4$ in 50 mL of 3/1 acetone/water and heating at reflux for 1 h. After the precipitated AgCl and $AgPF_6$ were filtered off, the volume of the resulting solution was reduced to 15 mL and 30 mL of saturated $NaClO_4$ added. The resulting precipitate was collected on a medium frit, washed with saturated $NaClO_4$ and three 1-mL portions of cold H_2O, and then air-dried. Yield: 315 mg; 91.6%.

The precipitate (160 mg) was purified further by elution from a Sephadex SP-C25-120 column with 0.1 M $NaClO_4$. A minor impurity eluted quickly followed by the desired complex. The resulting solution was reduced in volume by rotoevaporation at room temperature, the solution refrigerated overnight, and the resulting precipitate collected. Yield: 91 mg; 57%. Anal. Calcd for $C_{27}H_{22}N_5O_9Cl_2Ru$: C, 44.4; H, 2.9; N, 9.6. Found: C, 44.6; H, 3.1; N, 9.5.

[(trpy)(phen)Ru(O)]$(ClO_4)_2$. 0.204 mmol (150 mg) of [(trpy)(phen)Ru(H_2O)]$(ClO_4)_2$ was dissolved in a minimum amount of hot water. After filtration, the solution was cooled to room temperature. Bromine vapor was then bubbled through the solution, and a yellow solid immediately precipitated. A few milliliters of saturated $NaClO_4$ was added to complete precipitation while the solution was purged with N_2 to remove unreacted Br_2. The precipitate was collected on a medium frit, washed with a few drops of cold water, and dried in a vacuum desiccator.

[Ru(bpy)$_2$(2-pyOH)$_2$]$(PF_6)_2$ was prepared by stirring together for 1 h at room temperature 0.50 mmol (26 mg) of $[Ru(bpy)_2Cl_2]\cdot 2H_2O$ and 1.00 mmol (253 mg) of $AgPF_6$ in 25 mL of methanol. After 1 h, the methanol solution was filtered under N_2 into a flask containing 1 mmol (95 mg) of 2-hydroxypyridine (2-pyOH) and heated at reflux under nitrogen for 15 h in the dark. At the end of the reflux period, the solution was evaporated to dryness and the residue washed with water and air-dried. The solid was dissolved in CH_2Cl_2 and chromatographed on a 1 in. × 8 in. alumina column packed with CH_2Cl_2 containing 1% CH_3OH by volume. The percentage of CH_3OH was increased to 5% during elution until the compound was eluted as a red purple band. The solution was reduced in volume, the solid precipitated by addition to benzene, and the product dried in a desiccator overnight. Yield: 217 mg; 48%. Anal. Calcd for $C_{30}H_{26}N_6O_2RuP_2F_{12}$: C, 40.3; H, 2.9; N, 9.4. Found: C, 40.9; H, 2.4; N, 9.6.

[(bpy)$_2$(2-pyOH)Ru(H_2O)]$(PF_6)_2$. Into 15 mL of methanol was placed 50 mg of $[Ru(bpy)_2(2\text{-}pyOH)_2](PF_6)_2$. When solution was complete, 5 mL of 5% HPF_6/H_2O was added and the resulting solution was stirred for 30 min in room light and then reduced in volume. The room light is important since the reaction involved is a photochemical substitution for the pyridine ligand. The solid was collected in a 2-mL fritted funnel, washed well with chilled H_2O, and dried in a desiccator overnight. Yield: 26 mg; 57%. Anal. Calcd for $C_{25}H_{23}N_4O_2RuP_2F_{12}$: C, 36.8; H, 2.8; N, 8.6. Found: C, 36.9; H, 2.5; N, 8.9.

[(bpy)$_2$(2-pyO)Ru](PF$_6$). A 50-mg sample of $[Ru(bpy)_2(2\text{-}pyOH)_2](PF_6)_2$ was dissolved in 20 mL of absolute ethanol and stirred in room light for 30 min. The solution was evaporated to dryness, dissolved in CH_2Cl_2, filtered, and a solid was precipitated by addition to benzene. The solid was collected on a 2-mL fritted funnel, washed well with chilled H_2O, and dried in a desiccator overnight. Yield: 26 mg; 72%. Anal. Calcd for $C_{25}H_{20}N_5O_2RuPF_6$: C, 46.0; H, 3.10; N, 10.7. Found: C, 46.7; H, 2.9; N, 10.0.

Measurements. UV–vis. UV–visible spectra were recorded on a Bausch and Lomb Spectronic 2000 or a Hewlett Packard 8450A diode array spectrophotometer in quartz cells at room temperature.

Electrochemistry. Cyclic (CV) and differential-pulse (DPV) voltammetry were performed at room temperature by using a PAR Model 175 universal programmer and a PAR Model 173 potentiostat/galvanostat. Rotating disk electrode (RDE) measurements were performed by using a Pine Instrument Co. (Grove City, PA) Model ASR 2 rotator and Model RDE 3 potentiostat. Standard three-electrode circuitry was employed, with a Pt-wire counter electrode and saturated sodium calomel (SSCE) reference electrode. Potentials are reported vs. SSCE. A Luggin capillary was employed to minimize solution resistance effects in CH_2Cl_2. Teflon-shrouded Pt or glassy-carbon (0.0712 cm^2, GC-30, Tokai Carbon, Inc.) disk electrodes were used as working electrodes in aqueous solution; a Pt-button electrode was used in CH_2Cl_2. Values of n, where n is mol of electrons/mol of complex, were measured by exhaustive electrolysis at a constant potential, with a PAR Model 179 digital coulometer. A Pt-screen or reticulated vitreous carbon electrode, 12 holes/1 linear in. (ERG, Inc., Oakland, CA) was used in the coulometric determinations.

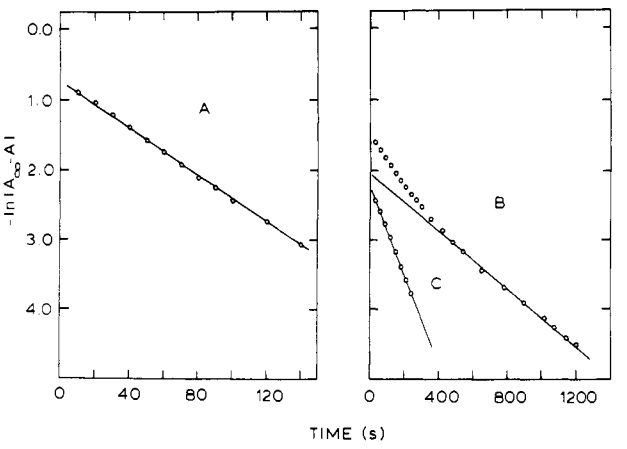

Figure 1. Plot of ln (absorbance change) vs. time at 510 nm for the reduction of (A) $[(trpy)(phen)Ru(O)]^{2+}$ at pH 12.8 and (B) $[(bpy)_2(py)Ru(O)]^{2+}$ at pH 12. (C) Plot of the differences between ln (absorbance change) and the linear portion of line B extrapolated to $t = 0$.

HPLC. HPLC experiments were performed on an IBM Model LC/9533 ternary gradient liquid chromatograph equipped with a UV-254-nm detector. The column used was a Partisil ODS-3 column from Whatman. Various mobile phases were used, which consisted of mixtures of solvent A (40% THF 60% 0.2 M acetate buffer, pH 3.6) and solvent B (5% THF; 95% 0.2 M acetate buffer, pH 3.6) or solvent C (40% THF; 60% 0.1 M trifluoromethanesulfonic acid, pH 2.6) and solvent D (5% THF; 95% 0.1 M trifluoromethanesulfonic acid, pH 2.6). All solvents were 5 mM in sodium octanesulfonate.

Gas Chromatography. Gas chromatography (GC) was performed with a 2-ft Al_2O_3 column chilled in acetone/dry ice with argon as carrier gas (30 psi).

Kinetics. Stopped-flow measurements were carried out on an Amin-co-Morrow stopped-flow apparatus attached to a Beckman DU monochromator, details of which are given elsewhere.[14] Conventional mixing experiments were performed on a Varian Series 634 instrument. Temperature was maintained to ±0.1 °C with a Forma Scientific Model 2095 temperature bath.

Kinetic Measurements on [(trpy)(phen)Ru(O)]$(ClO_4)_2$. Rate data for the apparent reduction of the oxo complex were obtained by monitoring absorbance changes at 320 and 510 nm. Initial concentrations of $[(trpy)(phen)Ru(O)]^{2+}$ in unbuffered solutions were varied from 2.90×10^{-5} to 1.45×10^{-4} M. Experiments were conducted under pseudo-first-order conditions with the hydroxide concentration ranging from 0.01 to 1.00 M. Ionic strengths were varied from 0.10 to 1.00 M with Na_2SO_4. Purging the reaction solutions with Ar prior to use had no apparent effect on the kinetics, so no attempt was made thereafter to use anaerobic conditions. First-order rate constants k were calculated on the basis of a least-squares fit (uniform weighting) to the relation

$$\ln |A_\infty - A_t| = -kt + \ln |A_t - A_0|$$

where A_∞ and A_0 are the final and initial absorbances, respectively. A_t is the absorbance measured at time t. Reactions were monitored to completion to obtain A_∞, and data from the first four half-lives were used in determining k. Rate constants obtained from replicate runs generally agreed within 5%.

Kinetic Measurements on [(bpy)$_2$(py)Ru(O)]$(ClO_4)_2$. Rate data were obtained by monitoring absorbance changes at 292, 312, 364, and 510

(12) Moyer, B. A.; Meyer, T. J. *Inorg. Chem.* **1981**, *20*, 436.
(13) Sullivan, B. P.; Calvert, J. M.; Meyer, T. J. *Inorg. Chem.* **1980**, *19*, 1407.
(14) Cramer, J. L. Ph.D. Dissertation, The University of North Carolina, Chapel Hill, NC, 1975, pp 191–216.

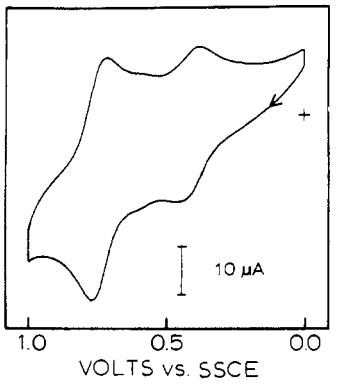

Figure 2. Cyclic voltammogram at a glassy-carbon electrode of the product of self-reduction of $[(bpy)_2(py)Ru(O)]^{2+}$ at pH 13 after acidification to pH 2 and removal of the crystalline portion. Potential scan rate was 0.05 V s^{-1}.

nm. The initial complex concentration was 0.10 mM. Experiments were conducted under pseudo-first-order conditions with the hydroxide concentration ranging from 0.01 to 0.10 M. Na_2SO_4 was used to maintain the ionic strength at 1.00 M. Absorbance vs. time data were plotted as ln (ΔA) vs. t, where ΔA is the absorbance change after time t (Figure 1). These plots had both a linear portion and an initial curved portion. By plotting the differences between the (ΔA) plot and the linear portion extrapolated to zero time vs. time, we obtained a straight line (Figure 1); the slope of this difference plot was taken to be the rate constant for the first reaction step.

Product Analysis. Products from the reduction of $[(trpy)(phen)Ru(O)]^{2+}$ and $[(bpy)_2(py)Ru(O)]^{2+}$ in base were determined by a combination of UV–vis spectroscopy, CV, and HPLC as outlined below for $[(bpy)_2(py)Ru(O)]^{2+}$. In one experiment, 0.006 g of $[(bpy)_2(py)Ru(O)]^{2+}$ was dissolved in 5 mL of distilled H_2O and then added to 5 mL of 0.20 M NaOH. After 2.5 h, the now reddish purple solution was acidified with 2 mL of concentrated $HClO_4$ and analyzed by CV. After 1 day (in the dark to avoid possible photoreactions), an orange solid precipitated. The solid was isolated and analyzed by UV–vis spectroscopy, CV, and HPLC. In another series of experiments, 5-mL aliquots of 10^{-4} M $[(bpy)_2(py)Ru(O)]^{2+}$ solution were added to equal volumes of 0.02 M NaOH. After various time intervals, ranging from 55 min to over 15 h, the reaction was quenched by adding 0.1 M triflic acid to pH 2.64. The resulting acidified solution was analyzed by UV–vis and HPLC.

Product Analysis from Electrolysis Experiments. In a typical electrolysis experiment, 10^{-5} mol of $[(trpy)(phen)Ru(H_2O)](ClO_4)_2$ was dissolved in 6 mL of 0.1 M NaOH and electrolyzed at 0.5 V using a reticulated vitreous carbon electrode in a three-arm electrolysis cell. After a given amount of charge was passed, electrolysis was interrupted and the solution subjected to analysis by CV using a glassy-carbon electrode placed in the working electrode compartment and HPLC or GC.

Results

Voltammetric Results. The major products of the spontaneous reductions of $[(trpy(phen)Ru(O)]^{2+}$ or $[(bpy)_2(py)Ru(O)]^{2+}$ in basic solution are the corresponding Ru(II) aquo complexes. UV–vis spectra of product solutions in base or after acid quenching are indistinguishable from authentic samples of the respective Ru(II) complexes under the same conditions. In addition, after acidification with $HClO_4$, a crystalline fraction can be separated from each product solution, which is identifiable as the corresponding Ru(II) aquo complex by UV–vis spectroscopy, CV, and HPLC. A cyclic voltammogram (Figure 2) of the product solution from $[(bpy)_2(py)Ru(O)]^{2+}$ reduction after the crystalline fraction has been removed shows three couples at $E^{\circ\prime}$ = 0.41, 0.58 (minor), and 0.74 V. The couple at the most positive potential arises from $[(bpy)_2(py)Ru(H_2O)]^{2+}$, which remained in the solution.

Illustrated in Figure 3 are results from acid quenching/HPLC experiments with $[(bpy)_2(py)Ru(O)]^{2+}$ after various reaction times at pH 12. Three products, I–III, in addition to $[(bpy)_2(py)Ru(H_2O)]^{2+}$ (at 13 min) appear early in the reaction. Peak I appears to grow as the reaction proceeds while the shoulder, II, subsides. Near the end of the reaction, I and III are still present, along with a new peak, IV. Similar experiments with $[(trpy)(phen)Ru(O)]^{2+}$ were not as well resolved as in Figure 3 but, along with the

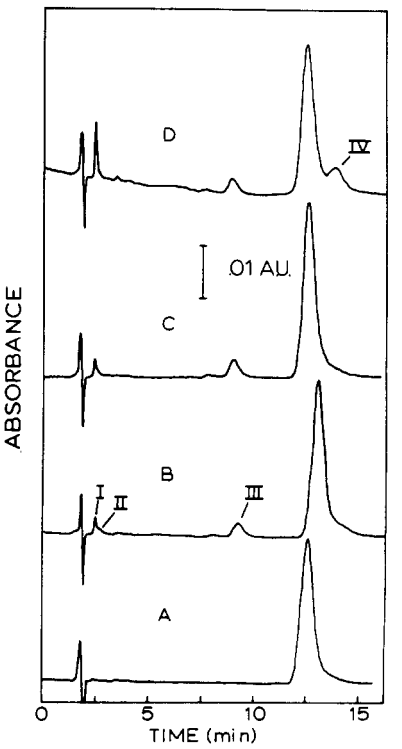

Figure 3. HPLC chromatogram of $[(bpy)_2(py)Ru(O)]^{2+}$ placed in 0.01 M NaOH and quenched with trifluoromethanesulfonic acid after (A) 0, (B) 55, and (C) 120 min and (D) 12 h: mobile phase, THF/0.1 M trifluoromethanesulfonic acid, 5 mM sodium octanesulfonate, 40/60 v/v; flow rate 1 mL/min; 250 × 4 mm Partisil ODS-3 column.

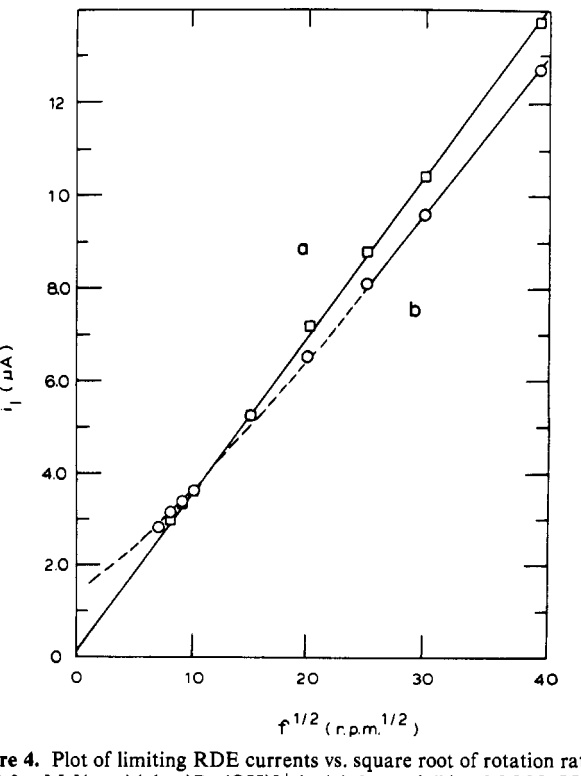

Figure 4. Plot of limiting RDE currents vs. square root of rotation rate for 0.2 mM $[(trpy)(phen)Ru(OH)]^+$ in (a) 0.1 and (b) 1.0 M NaOH. The surface area of the glassy-carbon electrode was 0.0712 cm^2.

experiments for $[(trpy)(phen)Ru(H_2O)]^{2+}$, are consistent with at least two and possibly four products after complete self-reduction. Aside from these voltammetric and HPLC observations, no further attempts were made to isolate or characterize the various products.

Rotating glassy-carbon disk electrooxidation of $[(trpy)(phen)Ru(OH)]^+$ was performed in 0.1 and 1.0 M NaOH.

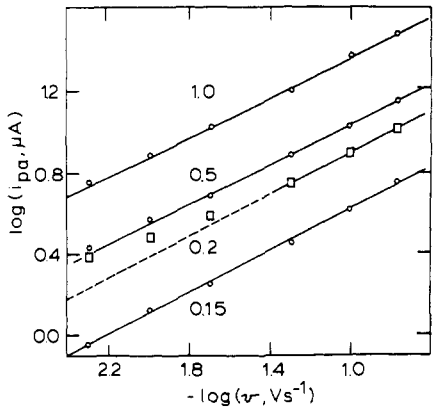

Figure 5. Dependence of the logarithm of the anodic peak current on the logarithm of the potential scan rate for the oxidation of [(trpy)(phen)-Ru(OH)]$^+$ in (○) 0.1 and (□) 1.0 M NaOH. [(trpy)(phen)Ru(OH)]$^+$ concentrations in mM are indicated by the numbers at each curve. The glassy-carbon electrode surface area was 0.0712 cm^2.

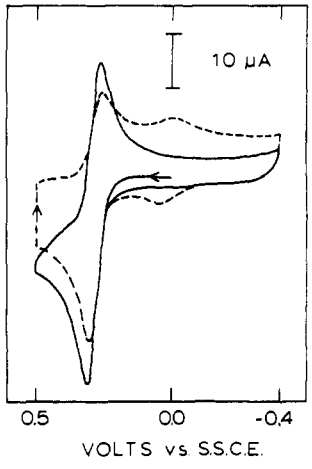

Figure 6. Cyclic voltammograms for 1 mM [(trpy)(phen)Ru(OH)]$^+$ in 0.1 M NaOH at glassy-carbon electrode: (—) initial scans; (--) scan after potential was held for 5 min at 0.5 V. The potential scan rate was 0.167 V s^{-1}, and the electrode surface area was 0.072 cm^2.

Limiting currents in 0.1 M NaOH obeyed the Levich equation, exhibiting a linear dependence on the square root of rotation rate with a zero intercept (Figure 4a). Limiting RDE currents were also proportional to concentration of the Ru(II) complex. However, in 1 M NaOH a curved Levich plot was observed at low rotation rates (Figure 4b); the form of the plot suggests that spontaneous self-reduction of [(trpy)(phen)Ru(O)]$^{2+}$ proceeds sufficiently rapidly that [(trpy)(phen)Ru(OH)]$^+$ is regenerated catalytically. At high rotation rates, Levich type behavior was regained. The linear Levich slopes of Figure 4 parts a and b (dashed line) give diffusion coefficients for [(trpy)(phen)Ru-(OH)]$^+$ of 4.6 × 10^{-6} and 4.3 × 10^{-6} cm^2/s in 0.1 and 1.0 M NaOH, respectively.

Cyclic voltammetry at glassy-carbon electrodes gave similar results. Peak currents for oxidation of [(trpy)(phen)Ru(OH)]$^+$ in 0.1 and 1 M NaOH gave logarithmic plots of current vs. potential scan rate with slopes close to 0.5 at high scan rate (Figure 5), as predicted for a diffusionally controlled process. However, in 1 M NaOH at lower potential scan rates, a similar deviation from linearity akin to that observed in the RDE experiment was observed (Figure 5).

When [(trpy)(phen)Ru(O)](ClO$_4$)$_2$ was dissolved in 0.1 M NaOH, the originally yellow solution turned to purple-red within a minute and the cyclic voltammogram of the resulting solution (not shown) was almost the same as shown for [(trpy)(phen)-Ru(OH)]$^+$ (Figure 6). The results of the experiment suggest that after one turnover the Ru(II) complex was formed almost entirely. By holding the potential of the electrode at 0.5 V for a few minutes, which maintains the complex in the Ru(IV) state at the electrode,

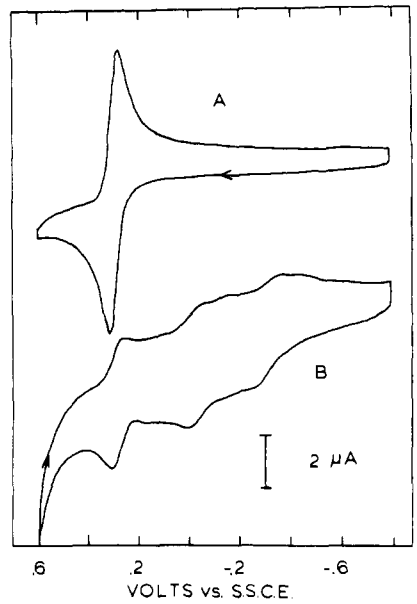

Figure 7. Cyclic voltammograms at glassy-carbon electrode of deoxygenated 2 mM [(trpy)(phen)Ru(OH)]$^+$ at pH 13, (A) before and (B) after 80 min of electrolysis at +0.5 V. The potential scan rate was 0.02 V s^{-1}.

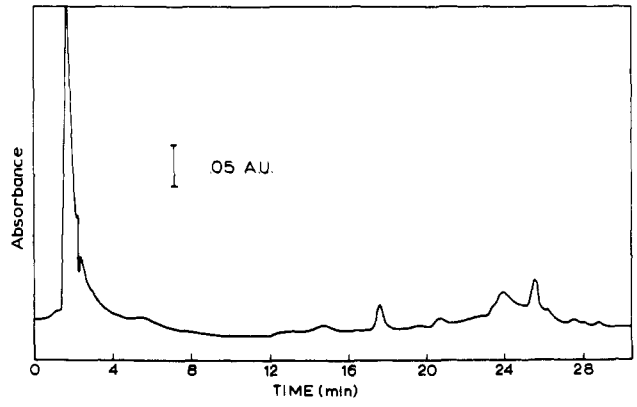

Figure 8. HPLC chromatogram of products of electrolysis at +0.5 V of [(trpy)(phen)Ru(OH)]$^+$ at pH 13: mobile phase, (A) THF/0.2 M acetic acid buffer pH 3.6, 5 mM sodium octanesulfonate, 40/60 v/v and (B) THF/0.2 M acetic acid buffer pH 3.6, 5 mM sodium octanesulfonate, 5/95 v/v; 2% A/min, flow rate 1.5 mL/min; 250 × 4 mm Partisil ODS-3 column.

we observed a new redox couple at $E^{o\prime}$ = 0.02 V (Figure 6, dashed line) and the current for oxidation of [(trpy)(phen)Ru(OH)]$^+$ was decreased. The new wave appears to arise from a primary product of the decomposition of electrooxidatively generated [(trpy)-(phen)Ru(O)]$^{2+}$. The same product also appears as a product of bulk electrolysis as noted below.

Electrolysis. O_2 production was not observed as a product of exhaustive, prolonged oxidative electrolysis of [(trpy)(phen)Ru-(H$_2$O)]$^{2+}$ in 0.1 M NaOH. Figure 7 illustrates the cyclic voltammogram of [(trpy)(phen)Ru(H$_2$O)]$^{2+}$ before and after electrolysis in a N_2-purged solution. In the potential window examined, seven new redox couples appear, having $E^{o\prime}$ = −0.58, −0.43, −0.31, −0.14, −0.02, 0.14, and 0.28 V. HPLC analysis of the oxidation products of a closely related experiment (Figure 8) show evidence for at least 14 products. Interpretation of the HPLC results is somewhat ambiguous since (1) the detection wavelength was 254 nm and non-Ru-containing organic products could also appear, and (2) since the solvents used for elution contained acetate, substitution of aquo ligands by acetate anion could add to the observed list of products. However, when coupled with Figure 7, the HPLC result clearly shows that the initial complex has undergone multiple redox transformations as a consequence of being oxidized to Ru(IV) in base.

Table I. Kinetic Data for the Spontaneous Reduction of $[(trpy)(phen)Ru(O)]^{2+}$ and of $[(bpy)_2(py)Ru(O)^{2+}]$ at Different Concentrations of OH^- at 26.2 °C, λ = 510 nm, and μ = 1.0 M (Na_2SO_4)

$[OH^-]$, M	10^5[Ru], M	10^2k_{obsd},[a] s^{-1}	$10k$, M^{-1} s^{-1}
	$[(trpy)(phen)Ru(O)]^{2+}$		
0.010	7.24	0.171	1.71
0.010	7.24	0.200	2.00
0.030	6.64	6.12	2.04
0.050	6.64	1.12	2.24
0.050	7.24	1.04	2.08
0.050	7.24	1.00	2.00
0.050[b]	7.24	1.15	2.30
0.070	6.64	1.57	2.24
0.100[c]	7.24	5.39	5.39
0.100	6.64	2.42	2.42
0.100	7.24	2.34	2.34
0.200	7.24	4.55	2.28
0.400	7.24	10.2	2.55
0.700	7.24	20.1	2.87
1.00	7.24	30.3	3.03
1.0	7.24	25.8	2.58
1.00	2.90	28.0	2.80
1.00	1.45	29.4	2.94
	$[(bpy)_2(py)Ru(O)]^{2+}$		
0.010	5.00	0.64[d]	0.64
0.010	5.00	0.20[e]	0.20

[a] Values are precise to ±5%. [b] Solutions purged with Ar. [c] μ = 0.1 M (Na_2SO_4). [d] k_{IV}. [e] k_{III}.

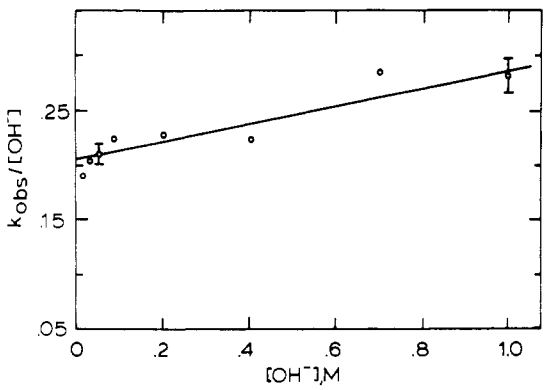

Figure 9. Plot of $k_{obsd}/[OH^-]$ vs. $[OH^-]$ concentration for the self-reduction of $[(trpy)(phen)Ru(O)]^{2+}$ in stopped-flow experiments.

Kinetics. The self-reduction of $[(trpy)(phen)Ru(O)]^{2+}$ was studied by the stopped-flow technique as a function of the concentration of added hydroxide ion, ruthenium complex, ionic strength, and temperature. Repetitive UV–vis scans in the range 850–300 nm at pH 12 show isosbestic behavior for well over 4 half-lives. As shown in the first-order plot, Figure 1A, $\ln|A_\infty - A_t|$ vs. time at 510 nm is linear; this behavior was observed at all hydroxide concentrations studied. No intermediates absorbing at low energies were detected at pH 12 or 13. Assuming that $d[Ru(II)]/dt = -d[Ru(IV)]/dt$, the experimental rate law can be described by

$$-d[Ru(IV)]/dt = [k_a[OH^-] + k_b[OH^-]^2][Ru(IV)] = k_{obsd}[Ru(IV)] \quad (1)$$

as shown by analysis of the kinetic results (Table I) as a plot of $k_{obsd}/[OH^-]$ vs. $[OH^-]$ (Figure 9). From the plot, k_a = 0.21 ± 0.01 M^{-1} s^{-1} and k_b = 0.08 ± 0.02 M^{-2} s^{-1} at 25 °C and μ = 1.0 M (Na_2SO_4). From the data in Table I an increase in ionic strength retards the reaction, and k_{obsd} is insensitive to a 5-fold change in Ru(IV) concentration. Activation parameters for the k_a path, determined from data collected at a series of temperatures (Table II), are $\Delta H^\ddagger$ = 12 ± 2 kcal/mol and $\Delta S^\ddagger$ = −20 ± 6 eu.

At pH 12 and 13 (μ = 1.0 M, Na_2SO_4), self-reduction of $[(bpy)_2(py)Ru(O)]^{2+}$ was slower and could be studied by conventional mixing techniques. As illustrated in Figure 1B, plots of $\ln|A_\infty - A_t|$ vs. time are not linear as shown by observations at 292, 312, 364, or 510 nm. Treating the absorbance–time data as arising from consecutive first-order reactions appears to be a good approximation (see Figure 1C). Regardless of the wavelength monitored, when the data were treated in this manner, the first portion of the reaction proceeds about three times faster than the second portion. At pH 13 (25 °C, μ = 1.0 M, Na_2SO_4) the observed rate constants are $k_1 = 6.4 \times 10^{-3}$ s^{-1} and $k_2 = 2.0 \times 10^{-3}$ s^{-1}. Figure 10 shows typical spectra during the self-reduction of $[(bpy)_2(py)Ru(O)]^{2+}$ in 0.10 M NaOH (μ = 1.0 M, Na_2SO_4). Most striking is the apparent appearance of $[(bpy)_2(py)Ru(OH)]^{2+}$ very early in the reaction as evidenced by the distinctive shoulder at 312 nm. The complex $[(bpy)_2(py)Ru(O)]^{2+}$ has λ_{max} = 300 nm with no shoulder at 312 nm.

Table II. Kinetic Data for the Reaction between $[(trpy)(phen)Ru(O)]^{2+}$ and OH^- at Different Temperatures[a]

T, °C	$[OH^-]$, M	10^2k_{obsd}, s^{-1}	$10k$, M^{-1} s^{-1}
38.6	0.03	1.99	6.63
38.6	0.05	3.46	6.92
38.6	0.07	4.59	6.56
38.6	0.10	6.40	6.40
14.7	0.03	0.316	1.05
14.8	0.05	0.635	1.27
14.8	0.07	0.912	1.30
14.8	0.10	1.02	1.02

[a] λ = 510 nm, μ = 1.0 M (Na_2SO_4), 7.6 × 10^{-5} M $[(trpy)(phen)Ru(O)]^{2+}$.

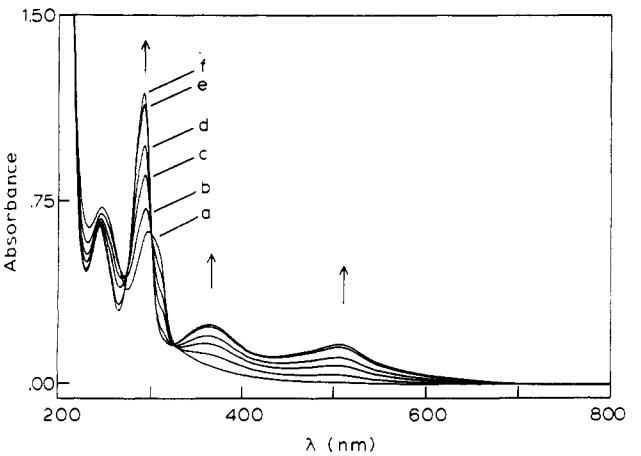

Figure 10. UV–vis spectra for $[(bpy)_2(py)Ru(O)]^{2+}$ at pH 13 recorded (a) 0, (b) 20, (c) 40, (d) 60, (e) 240, and (f) 480 s after placing the complex in solution.

Electronic Spectra. Electronic spectral data for the complexes of interest here are summarized in Table III.

$[(bpy)_2(pyOH)Ru(H_2O)]^{2+}$ (pyOH Is 2-Hydroxypyridine). The hydroxypyridine complex was prepared as a possible model for ligand-based oxidative hydroxylation, which appears to be the origin of the self-reduction. The complex was prepared according to the known scheme

$$2Ag^+ + Ru(bpy)_2Cl_2 \xrightarrow[-2AgCl]{\text{acetone (S)}} [Ru(bpy)_2(S)_2]^{2+} \xrightarrow[-2S]{pyOH} [Ru(bpy)_2(pyOH)_2]^{2+} \xrightarrow[H_2O]{h\nu} [Ru(bpy)_2(pyOH)(H_2O)]^{2+} + pyOH$$

to give the α-hydroxypyridine complex and/or its tautomer, the α-pyridone complex

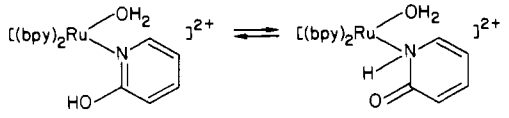

The similarity in the pattern of MLCT absorption bands for this complex compared, for example, with those of $[(bpy)_2(py)Ru-$

Table III. UV–Vis Electronic Absorption Data for the Ru Complexes[a]

complex	medium	λ_{max}, nm ($\epsilon \times 10^{-3}$)[b]
$[(bpy)_2Ru(pyOH)_2]^{2+}$ [c]	0.10 M H^+	514 (12.3), 347 (15.1), 295 (80.2), 247 (27.4)
	CH_3CN	505 (9.5), 341 (13.9), 292 (63.8), 245 (24.6)
$[(bpy)_2Ru(pyO)]^+$ [c]	CH_2Cl_2	514 (10.7), 347 (13.4), 294 (55.6), 245 (7.3)
$[(bpy)_2Ru(pyOH)(OH_2)]^{2+}$ [d]	0.10 M H^+	485 (7.7), 346 (8.3), 291 (56.7), 243 (24.8)
	0.10 M OH^-	493 (6.8), 349 (8.1), 293 (52.2), 244 (25.9)
$[(bpy)_2Ru(py)(OH_2)]^{2+}$ [e]	0.10 M H^+	470 (8.4), 335 (10.5), 290 (57.0), 243 (24.0)
$[(trpy)(phen)Ru(OH_2)]^{2+}$ [e]	0.10 M H^+	474 (9.6), 312 (34.1), 288 (35.1), 231 (24.9)
	0.10 M OH^-	510 (8.76), 318 (29.2), 291 (33.7), 275 (31.0), 235 (29.5)
$[(trpy)(phen)Ru(O)]^{2+}$ [e]	0.10 M H^+	325 sh (15.6), 311 (44.4), 284 (23.0), 275 sh (21.5)

[a] pyOH is 2-hydroxypyridine. [b] Molar extinction coefficients (±5%) are given in parentheses. [c] As PF_6^- salts. [d] As $CF_3SO_3^-$ salts. [e] As ClO_4^- salts.

$(H_2O)]^{2+}$ (Table III) suggests that the pyridone ligand is bound through the nitrogen atom and exists dominantly in the α-hydroxypyridine form. As noted above, if oxidative hydroxylation of pyridyl type ligands does occur, the hydroxy pyridine complex represents a model for the first stage of the reactions. In this regard, it is significant that oxidative electrolysis of $[(bpy)_2(pyOH)Ru(H_2O)]^{2+}$ in aqueous solution results in catalytic oxidative current in either acidic or basic solution.

An unexpected result worth noting is the appearance of 2-hydroxypyridine as a bidentate ligand, as a result of photolysis of the bis complex in absolute ethanol. The product

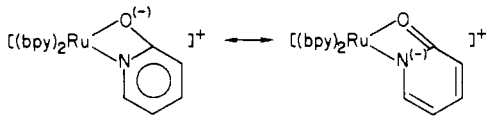

is the deprotonated chelate as shown by elemental analysis and solution conductivity data. When $[(bpy)_2Ru(pyO)]^+$ is dissolved in a coordinating solvent like CH_3CN or H_2O, the corresponding solvento complex appears as shown by the appearance of UV–vis λ_{max} and Ru(III)/Ru(II) $E_{1/2}$ values characteristic of the corresponding pyridine complex. In fact, the chelate may prove to be a useful synthetic intermediate for the introduction of a variety of ligands onto Ru(II).

pH Dependence of Reduction Potentials. As noted in earlier work based on polypyridyl aquo complexes of Ru and Os,[15] $E^{\circ\prime}$ values for the M(IV)/M(III) and M(III)/M(II) couples can be pH dependent because of the acid–base properties of aqua groups bound to M(II) and M(III). The results of pH-dependent $E_{1/2}$ measurements for the $[Ru(trpy)(phen)(H_2O)]^{2+}$ and $[Ru(bpy)_2(py)(H_2O)]^{2+}$ systems are shown in Figure 11. The results are presented as plots of $E_{1/2}$ vs. pH or Pourbaix diagrams. In the diagrams the pH-potential regions where one of the oxidation state components is of dominant stability are labeled. The vertical dashed lines represent pK_a values for the oxidation state components indicated. The lines show the potentials of the Ru(IV)/Ru(III) and Ru(III)/Ru(II) couples as a function of pH.

(15) Takeuchi, K. J.; Thompson, M. S.; Pipes, D. W.; Meyer, T. J. *Inorg. Chem.* **1984**, *23*, 1845.

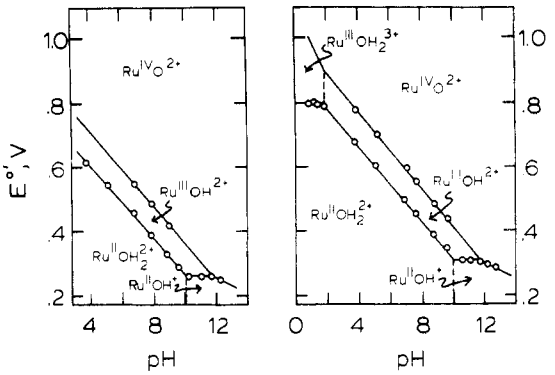

Figure 11. $E_{1/2}$ – pH (Pourbaix) diagram for the $[(bpy)_2(py)Ru(OH_2)]^{2+}$ (left) and $[(trpy)(phen)Ru(OH_2)]^{2+}$ (right) systems at $\mu = 0.1$ M and 22 ± 2 °C. The potential –pH regions of dominant stability for the three oxidation states are indicated as are pK_a values by the vertical dashed lines.

pK_a data and $E^{\circ\prime}$ values at pH 7 are compared in Table IV for three closely related systems for which data are available. Note the similarity in values between $[(trpy)(phen)Ru(OH_2)]^{2+}$ and $[(trpy)(bpy)Ru(OH_2)]^{2+}$, suggesting the interchangeability of the *bpy* and *phen* ligands. Note also that there are slight differences from the other two for the $[(bpy)_2(py)Ru(OH_2)]^{2+}$ system. Some variations in pK_a values with ionic strength are evident for all three systems, as expected.

From Figure 11, in basic solution the potentials for the Ru(IV)/Ru(III) and Ru(III)/(II) couples cross because of the different pH dependences for the two couples

$$Ru^{IV}\text{–}O^{2+} + H^+ + e^- \rightarrow Ru^{III}\text{–}OH^{2+} \quad E^{\circ\prime}(IV/III)$$

$$Ru^{III}\text{–}OH^{2+} + e^- \rightarrow Ru^{II}\text{–}OH^+ \quad E^{\circ\prime}(III/II)$$

Past the crossing point, which occurs, for example, at pH 12 for $[(trpy)(phen)Ru(OH_2)]^{2+}$, Ru(III) is unstable with respect to disproportionation, $2Ru^{III}\text{—}OH^{2+} \rightarrow Ru^{IV}\text{=}O^{2+} + Ru^{II}\text{—}OH^+ + H^+$, and the only observable redox process at the electrode is the 2-electron Ru(IV)/Ru(II) couple

$$H^+ + 2e^- + Ru^{IV}O^{2+} \rightarrow Ru^{II}\text{–}OH^+$$

In principle, in even stronger base, deprotonation of Ru(III) would occur, $RuOH^{2+} + OH^- \rightarrow RuO^+$. In this domain the Ru(III)/Ru(II) couple would become pH independent, and it is conceivable that in a strongly basic environment Ru(III) might reappear as a stable oxidation state.

A seemingly minor difference between the pK_a values (at 1.0 M ionic strength) for the $[(bpy)_2(py)Ru(OH_2)]^{2+}$ and $[(trpy)(phen)Ru(OH_2)]^{2+}$ complexes points to a subtle difference in their self-reduction behaviors. $[(trpy)(phen)Ru^{III}(OH)]^{2+}$ is, according to the pK_a data, unstable with respect to disproportionation above pH 12; correspondingly it does not appear as a product in the kinetic studies. On the other hand, $[(bpy)_2(py)Ru^{III}(OH)]^{2+}$ is stable to almost pH 13, and it does appear as a product.

Discussion

Self-Reduction of $[(trpy)(phen)Ru(O)]^{2+}$ and $[(bpy)_2(py)Ru(O)]^{2+}$. As noted in the introduction, recent studies of the self-reductions of tris(polypyridyl) complexes of Fe(III)[11] and Ru(III)[10] in basic solution, provide a convenient basis for comparison to self-reductions by $[(trpy)(phen)Ru(O)]^{2+}$ and $[(bpy)_2(py)Ru(O)]^{2+}$ under comparable conditions. Nord and co-workers[11] do observe O_2 production upon addition of $[Fe(phen)_3]^{3+}$ or $[Fe(bpy)_3]^{3+}$ to strongly basic solutions. They suggest that the rate-determining step is hydroxide attack on the metal center, followed by rapid formation of ligand-based *N*-oxide products bound to Fe(II). In the presence of $[(LL)_2Fe(OH)_2]^+$ (LL = bpy or phen), O_2 evolution is observed with recovery of 85–95% of $[Fe(LL)_3]^{3+}$ as $[Fe(LL)_3]^{2+}$.

The chemistry of $[Ru(bpy)_3]^{3+}$ in base is distinctly different from its first-row analogue in that only a trace amount of O_2 is formed. Creutz and Sutin[16] and Ghosh et al.[10] have shown that

Table IV. Reduction Potentials at pH 7 vs. SSCE and pK_a Values (23 °C)

Ru(IV)/Ru(III)/Ru(II) couples	μ, M	$E_{1/2}$, V (IV)/(III)	$E_{1/2}$, V (III)/(II)	pK_a Ru^{III}–OH_2^{3+}	pK_a Ru^{II}–OH_2^{2+}
$[(bpy)_2(py)Ru^{IV}(O)]^{2+}/[(bpy)_2(py)Ru^{III}(OH)]^{2+}/[(bpy)_2(py)Ru^{II}(OH_2)]^{2+}$ [a]	1.0	0.53	0.42	0.85	10.80
	0.1	0.54	0.44	0.85	10.20
$[(trpy)(phen)Ru^{IV}(O)]^{2+}/[(trpy)(phen)Ru^{III}(OH)]^{2+}/[(trpy)(phen)Ru^{II}(OH_2)]^{2+}$	1.0	0.58	0.48	...	10.2
	0.1	0.60	0.50	1.7	10.0
$[(trpy)(bpy)Ru^{IV}(O)]^{2+}/[(trpy)(bpy)Ru^{III}(OH)^{2+}/[(trpy)(bpy)Ru^{II}(OH_2)]^{2+}$ [b]	0.1	0.62	0.49	1.7	9.7

[a] Data from ref 12 and 17. [b] Data from ref 15. [c] Ionic strength maintained with Na_2SO_4.

the reduction of $[Ru(bpy)_3]^{3+}$ to $[Ru(bpy)_3]^{2+}$ is enhanced at high pHs and conclude that the rate-determining step involves "pseudo-base formation" in which OH^- is added to a carbon atom of the ligand

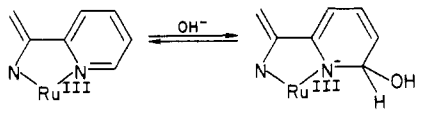

They also suggest that pseudo-base formation is followed by rapid, intramolecular electron transfer

$$[(bpy)_2Ru^{III}(^{(-)}bpyOH)]^{2+} \rightarrow [(bpy)_2Ru^{II}(\cdot bpyOH)]^{2+}$$

which, in turn, is followed by a rapid, ligand-based oxidation using $[Ru(bpy)_3]^{3+}$ as the oxidant

$$[(bpy)_2Ru^{II}(\cdot bpyOH)]^{2+} \xrightarrow[-H^+]{[Ru(bpy)_3]^{3+}} [(bpy)_2Ru^{II}(py\text{–}pyOH)]^{2+}$$

In the equation above py–pyOH is used as an abbreviation for the mixed pyridine–hydroxypyridine ligand, which is expected to be the initial oxidation product. In a redox cycle, ca. 10% of the original $[Ru(bpy)_3]^{3+}$ complex is degraded to several modified, $[Ru(bpy)_3]^{2+}$-like complexes in which varying degrees of ligand oxidation have occurred. The appearance of a high percentage of unmodified $[Ru(bpy)_3]^{2+}$ as product and of a series of ligand-oxidized products are significant observations. They suggest that, past the initial oxidation stage, the intermediates that appear are activated toward further oxidation. In this context, our observation of catalytic current in the oxidative electrolysis of $[(bpy)_2(pyOH)Ru^{II}(OH_2)]^{2+}$ over a broad pH range is notable.

Given the absence of O_2 formation in the self-reductions of $[(trpy)(phen)Ru(O)]^{2+}$ and $[(bpy)_2(py)Ru(O)]^{2+}$ in basic solution, the concurrent formation of several Ru-containing products, and the high yield of $[(trpy)(phen)Ru(H_2O)]^{2+}$ or $[(bpy)_2(py)Ru(H_2O)]^{2+}$, we conclude that the redox chemistry observed here is also ligand-based.

With the earlier results in mind, we suggest that the following are reasonable conclusions concerning the products and perhaps even the mechanistic details of the reduction of the Ru^{IV}–oxo complexes in basic solution. For the self-reductions of $[(trpy)(phen)Ru(O)]^{2+}$ and $[Ru(bpy)_3]^{3+}$, $\Delta S^{\ddagger} = -20$ and 7 eu, respectively. The positive entropy of activatiion for the self-reduction of $[Ru(bpy)_3]^{3+}$ is at least consistent with hydroxide addition to the ligand as the rate-determining step because of the decrease in total charge involved. The relatively large *negative* value of $\Delta S^{\ddagger}$ for the oxo complex is in marked contrast and signals a difference between the two cases in the rate-determining step. For the oxo complex the rate-determining step may be the redox step following pseudo-base formation

$$OH^- + [(trpy)(phen)Ru^{IV}(O)]^{2+} \rightarrow [^{(-)}trpyOH)(phen)Ru^{IV}(O)]^{+} \xrightarrow{slow} [(trpyOH)(phen)Ru^{II}(OH)]^{+}$$

where either trpy- or phen-based ligand oxidation products are possible. This mechanistic suggestion is at least consistent with our inability to observe an intermediate analogous to $[(bpy)_2Ru^{II}(\cdot bpyOH)]^{2+}$, which absorbs at λ_{max} = 700–800 nm.

However, the details of the rate-determining step are open to speculation. It is conceivable that a one-electron, intramolecular electron transfer occurs from the hydroxylated ligand to the Ru(IV) followed by a second, rapid inter- or intramolecular electron transfer to Ru(III)

$$[(^{(-)}trpyOH)(phen)Ru^{IV}(O)]^{+} \rightarrow [(\cdot trpyOH)(phen)Ru^{III}(OH)]^{+} \xrightarrow{fast} [(bpy\text{–}pyOH)(phen)Ru^{II}(OH)]^{+}$$

Under comparable conditions $[Ru(bpy)_3]^{3+}$ undergoes self-reduction with k = 150 M^{-1} s^{-1}, compared with k = 0.21 M^{-1} s^{-1} for the oxo complex. The enhanced reactivity for $[Ru(bpy)_3]^{3+}$ would certainly be understandable on the basis of an intramolecular electron-transfer mechanism given the fact that the Ru^{III} site in $[Ru(bpy)_3]^{3+}$ is more strongly oxidizing at pH 12 than the Ru^{IV}=O site by more than 1 V. Note, however, that in the self-reduction of $[Ru(bpy)_3]^{3+}$, the rate-determining step precedes electron transfer and as such the value of 150 M^{-1} s^{-1} is best regarded as a lower limit for the rate of intramolecular electron transfer. Presumably, a Ru(III)–radical intermediate would quickly undergo a second, one-electron, intramolecular electron transfer.

For $[(trpy)(phen)Ru(O)]^{2+}$, $[(trpy)(phen)Ru^{II}(OH)]^{+}$ would be the *initial* product observed in any case because Ru(III) is unstable with respect to disproportionation. By the same token, in the self-reduction of $[(bpy)_2(py)Ru(O)]^{2+}$, Ru(III) appears as a product, but since Ru(III) is stable with respect to disproportionation, its origin could be in the rapid comproportionation reaction between Ru(IV) and Ru(II) to give Ru(III).[17] It is interesting to note that, because of the buildup of Ru(III), biphasic kinetic plots are observed for $[(bpy)_2(py)Ru(O)]^{2+}$ because self-reduction of the Ru(III) complex follows self-reduction of Ru(IV).

A second possibility for the intramolecular redox step is that it involves a 2-electron, intramolecular hydride transfer to give the hydroxypyridine directly

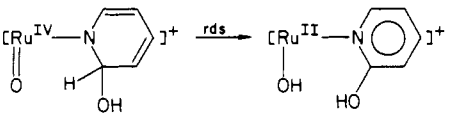

Hydride-transfer or hydride-transfer-like pathways have been invoked for these oxidants with other substrates. The large negative $\Delta S^{\ddagger}$ value for the self-reduction of $[(trpy)(phen)Ru(O)]^{2+}$ is reminiscent of activation parameters obtained for paths thought to occur by hydride transfer (as well as one-electron, hydrogen atom pathways).[4-6]

In considering steps past the initial oxidation stage, it is worth returning to the redox characteristics of the α-hydroxypyridine complex, $[(bpy)_2(pyOH)Ru(OH_2)]^{2+}$. Two points of note are the instability toward further oxidation at the ligand, even at the Ru(III) stage, over an extended pH range. The second is the marked decrease in potential for the Ru(II) → Ru(III) oxidation (0.64 V at pH 1.1) for the α-hydroxypyridine complex compared to that for the pyridine complex (0.78 V at pH 1.1). It is interesting to note that product waves arising from self-reduction of $[(bpy)_2(py)Ru(O)]^{2+}$ and $[(trpy)(phen)Ru(O)]^{2+}$ also occur

(16) Creutz, C.; Sutin, N. *Proc. Natl. Acad. Sci. U.S.A.* **1975**, *72*, 2858.

(17) Binstead, R. A.; Moyer, B. A.; Samuels, G. J.; Meyer, T. J. *J. Am. Chem. Soc.* **1981**, *103*, 2897.

in this potential region, suggesting that hydroxypyridine type species may also appear as intermediates, at least, in the initial stage of ligand oxidation.

The decrease in Ru(III)/Ru(II) potential following ligand oxidation also helps to explain why the majority of reduced product is the reduced, unmodified complex. Following reduction via pyridyl group hydroxylation

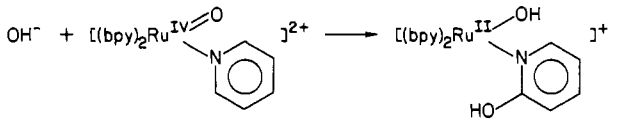

the hydroxypyridine Ru(II) complex would be rapidly oxidized to Ru(III) by either $[(bpy)_2(py)Ru^{IV}(O)]^{2+}$ or $[(bpy)_2(py)Ru^{III}(OH)]^{2+}$, leading to unmodified, reduced complex product and further ligand oxidation of $[(bpy)_2(pyOH)Ru(O)]^{+}$.

Final Comments. A goal of this work was to evaluate the ability of polypyridyl ruthenium oxo complexes to act as oxidation catalysts in basic solution. It is clear that some catalyst loss occurs as a result of competitive ligand oxidation processes that are enhanced in regions of high pH. For example, $[(bpy)_2(py)Ru(O)]^{2+}$ is stable toward self-reduction in acidic or neutral solution for hours while at pH 13 the half-time for self-reduction is 2 min. Nonetheless, the rates observed here for the self-reduction processes are sufficiently slow that useful catalytic rate data can be obtained in basic solution[9] provided the substrate of interest is sufficiently reactive and/or present in large excess.

Acknowledgment. This research was supported in part by grants from the National Science Foundation to Thomas J. Meyer under Grant No. CHE-8304230 and to Royce W. Murray under Grant No. CHE-7920114.

Registry No. **1**, 67202-43-1; **2**, 98542-34-8.

Contribution from the Chemistry Department,
Royal Veterinary and Agricultural University, DK-1871 Copenhagen V, Denmark

Ammonia Scrambling as a Result of Chloride Photoaquation in Chloropentaamminerhodium(III)

L. H. SKIBSTED

Received March 19, 1985

The ^{15}N-labeled compounds *cis*- and *trans*-$[Rh(NH_3)_4(^{15}NH_3)Cl]Cl_2$ have been prepared. The ammonia ligand that is photoaquated in aqueous perchloric acid solution at 13 °C as a result of ligand field excitation of labeled $Rh(NH_3)_5Cl^{2+}$ originates to an equal extent from axial and equatorial positions, implying that the axial ammonia is labilized four times as efficiently as the equatorial ammonia ligands. The axial/equatorial ammonia photoaquation ratio shows no significant temperature dependence up to 37 °C. Isotopic analyses of the ammonia that is photoaquated from labeled $Rh(NH_3)_5Cl^{2+}$ in acidic aqueous chloride solution showed that chloride photoaquation and subsequent photoanation result in ammonia scrambling.

Introduction

Ligand field excitation of hexacoordinated rhodium(III) ammine complexes leads to ligand labilization and, in aqueous solution, to photoaquation with relatively large, wavelength-independent quantum yields.[1,2] In complexes belonging to the pentaammine series, the ammonia that becomes substituted by water as a result of ligand field excitation can originate either from the axial position on the tetragonal axis or from an equatorial position. Such excited-state substitution reactions have high stereomobility,[3-5] and the product stereochemistry is not necessarily indicative of whether axial or equatorial ammonia is substituted:

$$Rh(NH_3)_5I^{2+} + H_3O^+ \xrightarrow{h\nu} \textit{trans}\text{-}Rh(NH_3)_4(H_2O)I^{2+} + NH_4^+$$

$$Rh(NH_3)_5(CN)^{2+} + H_3O^+ \xrightarrow{h\nu} \textit{cis}\text{-}Rh(NH_3)_4(H_2O)(CN)^{2+} + NH_4^+$$

However, for cyanopentaamminerhodium(III) a direct indication of specific equatorial photolabilization has been obtained by ^{15}N-labeling.[6] The ammonia photoaquation in this latter complex in which, notably, the heteroligand is the stronger field ligand, is thus occurring by a stereoretentive process. In order to establish the origin of the photolabilized ammonia in a pentaamminerhodium(III) complex containing a ligand of weaker field than ammonia, chloropentaamminerhodium(III) has been ^{15}N-labeled. The labeling procedures are reported here together with a photochemical investigation of the two substrates *cis*- and *trans*-$Rh(NH_3)_4(^{15}NH_3)Cl^{2+}$.

Experimental Section

Materials. $[Rh(NH_3)_5Cl]Cl_2$ was prepared according to a published procedure,[7] 99% ^{15}N-enriched NH_4Cl was supplied by Amersham Int., and other reagents were of analytical grade.

Spectra. Electronic absorption spectra were recorded on a Cary Varian 219 spectrophotometer.

Isotopic Analysis. The ^{15}N isotopic abundance in the labeled compounds and in the photochemically liberated NH_3 was determined by optical emission analysis at the Physics Laboratory of the Royal Veterinary and Agricultural University. A detailed description of the analytical procedure may be found in ref 8.

Photolysis Experiments. Weighed amounts of the labeled compounds were dissolved in 50-mL aliquots of the appropriate acidic aqueous media. The resulting solutions were transferred to quartz tubes and irradiated with 350-nm light in a Rayonet RMR-500 photochemical reactor. The light intensity was approximately 3×10^{12} quanta mL^{-1} s^{-1}. The photolysis solutions were stirred magnetically and temperature was kept

(1) Ford, P. C. *Coord. Chem. Rev.* **1982**, *44*, 61.
(2) Ford, P. C.; Wink, D.; DiBenedetto, J. *Prog. Inorg. Chem.* **1983**, *40*, 213.
(3) Sexton, D. A.; Skibsted, L. H.; Magde, D.; Ford, P. C. *Inorg. Chem.* **1984**, *23*, 4533.
(4) Mønsted, L.; Skibsted, L. H. *Acta Chem. Scand., Ser. A* **1983**, *A37*, 663.
(5) Mønsted, L.; Skibsted, L. H. *Acta Chem. Scand., Ser. A* **1984**, *A38*, 535.
(6) Svendsen, J. S.; Skibsted, L. H. *Acta Chem. Scand., Ser. A* **1983**, *A37*, 443.
(7) Hancock, M. P.; Nielsen, B.; Springborg, J. *Inorg. Synth.*, in press.
(8) Johansen, H. S.; Middelboe, V. *Appl. Spectrosc.* **1982**, *36*, 221.

0020-1669/85/1324-3791$01.50/0